The Detailed Model of the Middle Finger Extensor Mechanism for Understanding the Role of Intercrossing Fibers

Anton Dogadov, Francisco Valero-Cuevas, Christine Serviere, Franck Quaine

The Detailed Model of the Middle Finger Extensor Mechanism for Understanding the Role of Intercrossing Fibers

Anton Dogadov[1], Francisco Valero-Cuevas[2], Christine Serviere[1], Franck Quaine[1]

[1] Univ. Grenoble Alpes, GIPSA-Lab, F-38000 Grenoble, France

CNRS;GIPSA-Lab, F-38000 Grenoble, France

[2]Brain-Body Dynamics Lab, University of Southern California, Los Angeles, USA

Abstract: The extensor mechanism is a tendinous structure playing an important role in finger movement. It transmits the forces from several intrinsic and extrinsic muscles to multiple tendinous attachment points. The most important attachment points are located at the base of the second and third phalanx (proximal and distal attachments). The extrinsic muscle controls the force in proximal attachment by medial extensor mechanism band and intrinsic muscles control the force in distal attachment by lateral bands. Moreover, there exists two layers of intercrossing fibers, connecting medial band with the lateral ones. Intercrossing fibers transmits a fraction of the extrinsic muscle force to the proximal attachment and a fraction of the intrinsic muscle force to the distal one. In the current study, a numerical model of the extensor mechanism was built to analyze the role of intercrossing fibers in force transmission. The full extensor mechanism model containing the intercrossing fibers was compared with a trivial model, containing no connecting tissue between the medial and lateral bands. It was shown that the intercrossing fibers can play an important role in force transmission, modifying the force distribution among the extensor mechanism bands according to loading and posture. Influence of the intercrossing fiber parameters on force transmission was also demonstrated.

Keywords: Finger, Tendons, Extensor apparatus, Extensor mechanism, Extensor assembly

Introduction

The extensor mechanism (EM) of the finger is a tendinous structure, situated at the dorsal surface of the finger bones and transmitting the force from several extrinsic and intrinsic hand muscles to finger joints (Landsmeer, 1949). This structure is presented in human hands, as well as in the hands of primates (Van Zwieten, 1980). The extensor mechanism plays and important role in finger movement and is usually included into biomechanical models of the finger (Hu et al., 2014; Sachdeva et al., 2015; Synek and Pahr, 2016; Valero-Cuevas et al., 2007; Vaz et al., 2015). In the current study, we focus, without loss of generality, on the EM of the middle finger. This mechanism principally consists of

1. A medial tendon which stars from the *extensor digitorum communis III* muscle and has principal bone attachment at the proximal part of the second phalanx (medial tendon) (Harris and Rutledge, 1972);
2. Two lateral bands (or intrinsic), radial and ulnar, which start from intrinsic muscles. Radial and ulnar radial band combine and attach to the proximal part of the third phalanx (terminal tendon) (Harris and Rutledge, 1972);
3. Intercrossing fibers, connecting the lateral bands with the medial one (Schultz et al., 1981).

The medial extensor tendon passes through the proximal interphalangeal joint (PIP) and terminal extensor tendon passes through the distal interphalangeal joint (DIP), creating moments in them. The intercrossing fibers are of the particular interest, because they make the forces in medial and terminal tendon biomechanically dependent, and, hence, couple the movement in both interphalangeal joints (Leijnse and Spoor, 2012). Moreover, the intercrossing fibers way become more tight or slack as a function of the posture (Leijnse and Spoor, 2012), making the force transmission among the extensor mechanism bands posture dependent (Lee et al., 2008; Sarrafian et al., 1970). It was also shown that the extensor mechanism shows nonlinear "switching" behavior (Valero-Cuevas et al., 2007). It means that the force transmission among the EM bands depends on the input muscle forces. However, there is a lack of studies analyzing the role of intercrossing fibers in force transmission among the extensor mechanism bands.

The purpose of this study was to complete this gap by studying the effects of the intercrossing fiber layers on force transmission among the EM bands and on an output fingertip force. For this purpose, we built and compared two three-dimensional models of the extensor mechanism: a full model, including the intercrossing fibers and an extensor hood, and a trivial model, without any structures connecting the central band with the laterals ones.

The results of this study give the information about the variation of the force transmission in finger extensor mechanism with posture and force, introduced by the intercrossing fibers. This information may be important for better understanding evolutionary advantages of such a topology of the extensor mechanism, in which the central and lateral bands are connected by the intercrossing fibers in comparison with such a topology of the extensor mechanism, in which the force in terminal and medial tendons are biomechanically independent. The results of this study may also help understanding the neuromuscular strategies of finger control.

Methods

Model

The computational environment for the extensor mechanism (EM) modeling was created using Matlab 2015 and C++ and was based on the extensor mechanism simulator, presented in (Dogadov et al., 2017). This environment allows simulating the EM with different topologies for different muscle forces and fingertip posture. The environment allows only static simulations, *i.e.* it is may be used to calculate the forces in tendons as well as the fingertip force for a given fixed posture and muscle forces.

To study the effect of intercrossing fibers, we compared two models, with and without them. The first model (Fig. 1a) was a full EM model, containing the main EM tendons: extensor medial band (5), connecting the extrinsic *extensor digitorum* muscle with the medial extensor tendon (*me*-tendon, 6), which forms a proximal attachment of the EM to the skeleton; the lateral (or interosseous) bands (4), connecting the intrinsic muscles with terminal extensor tendon (*te*-tendon, 10) which forms a proximal attachment of the EM to the skeleton. The model also contain the structures, connecting the lateral band

with the medial one. These structures are the extensor hood (1), the intrinsic medial fibers (*im*-fibers, 2, shown in red) and the extensor lateral bands (*el*-fibers, 3, shown in blue). The second model was the trivial one, with no structures connecting the lateral tendons with the medial one. The transverse retinacular ligament (7) and triangular ligament (8) were included to both models. The attachment points of the tendons and ligaments to bones are shown by circles.

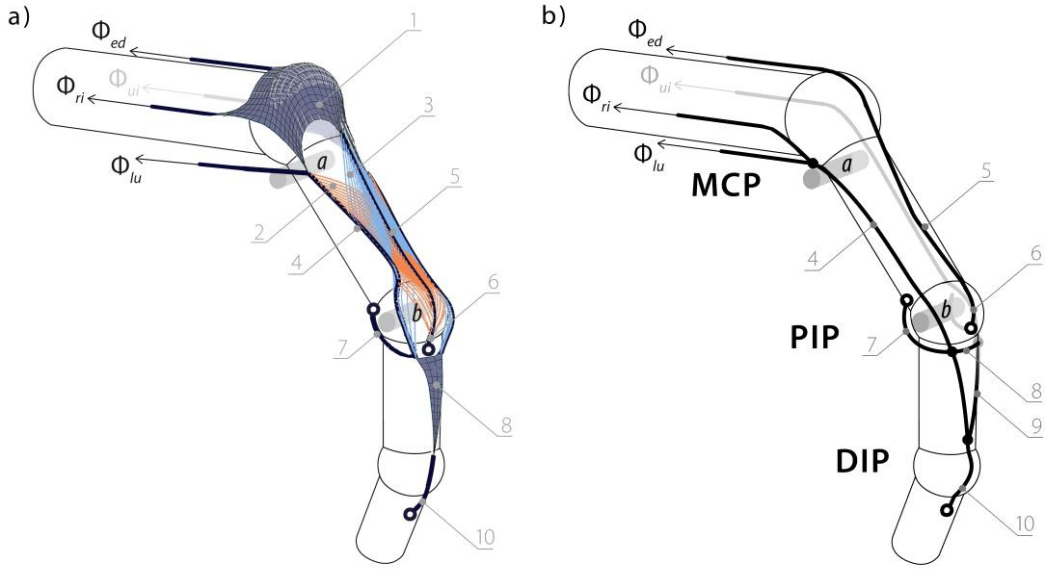

Fig. 1. The view of the extensor mechanism modelled in a developed environment. a:the full model, which contains the principal tendon and ligaments of the extensor mechanism: 1 – the extensor hood, 2 – interosseous medial fibers (red), 3 – the extensor lateral fibers (blue), 4 – lateral band, 5 – extensor medial band, 6 – medial extensor tendon, 7 – transverse retinacular ligament, 8 – triangular ligament, 10 – terminal extensor tendon. b: the trivial model. The trivial model does not contain the structures connecting the lateral bands(4) with the extensor medial band (5). The triangular ligament is represented by elements 8 and 9.

The developed environment allows representing the EM by principal building blocks: strings (shown with black in Fig. 1), membranes (violet) and fiber layers (red and blue). Each building block consist of a sequence of points, pairwise connected by elastic elements with a linear stress-strain model.

The extensor mechanism was placed on the finger bones in initial configuration according to anatomical data (Garcia-Elias et al., 1991).. The skeleton model included metacarpal bone (*mc*), proximal, intermediate and distal phalanx of the middle finger (p_1, p_2, p_3). Hence, the finger joints, considered by the model were a metacarpal (MCP), proximal interphalangeal (PIP), and distal interphalangeal (DIP) joint. The bones were represented by ideal cylinders the cylinders with the spheres at the ends. The geometrical parameters of the cylinders and spheres were adjustable. In current study the cylinder diameters were 64.6 mm, 44.6 mm, 26.3 mm, 17.4 mm; the cylinder radii 4.5 mm, 4.0 mm, 3.0 mm, 2.5 mm; the sphere radii were 5.0 mm, 5.4 mm, 4 mm for both models.

In addition to bones, two cylinders (*a*, *b* in Fig. 1) with smaller radii were included to the model to avoid the tendon bowstringing. The cylinder *a* is perpendicular to a *mc*-bone and replaces the functions of

the lumbrical muscle pulley (Stack, 1963); the cylinder *b* is perpendicular to p_1-bone and replace the function of the protuberances of p_1 head.

The force of the *extensor digitorum communis* muscle (EDC), ulnar and radial *interosseous* muscle (UI, RI), and lumbrical muscle (LU) were applied to the EM model as the input forces. We will note the muscle force values as vector **Φ**:

$$\mathbf{\Phi} = \left[\Phi_{ed} \;\; \Phi_{ui} \;\; \Phi_{ri} \;\; \Phi_{lu}\right]^T .$$

The deformation of the extensor mechanism due to the applied forces and geometrical constraints, imposed by the bones and the cylinders *a* ,*b* was performed to minimize the overall potential energy of all elastic elements by a gradient algorithm until the equilibrium state was found, as described in (Dogadov et al., 2017).

Once the equilibrium state of the extensor mechanism was found for a set of applied forces, the internal tendon forces as well as the output fingertip force was calculated. The internal tendon forces were found from the deformed EM model using the elongation of the elastic elements and their stiffness. The forces, transmitted from the EM to the bones, including the forces in tendinous attachments as well as the contact forces, were used to calculate the moments in joints. The moments created by the EM were calculated about all axis allowing the movement (two axis for MCP and one for PIP and PIP).The output fingertip force was found as a product of the finger Jacobian, defined by the finger geometry and a posture, with the joint moment vector. This approach is explained in (Valero-Cuevas, 2015).

Two EM models were compared to study the contribution of the intercrossing bands to nonlinear properties of the extensor mechanism, the variation of the force transmission with posture and activation level.

Study of the intercrossing bands

Study of the linearity of the extensor mechanism with reference to the input forces

To characterize the switching behavior of the extensor mechanism we studied he linearity of the extensor mechanism model with reference to the input forces. Firstly, extrinsic EDC muscle and interosseous muscle force (UI, RU, and LU) were applied to the EM models individually, and secondly, all four muscle forces were applied to EM-model at the same time:

$$\left[0 \;\; \Phi^{\max} \;\; 0 \;\; 0\right]^T \;\; \left[\Phi^{\max} \;\; 0 \;\; \Phi^{\max} \;\; \Phi^{\max}\right]^T \;\; \left[\Phi^{\max} \;\; \Phi^{\max} \;\; \Phi^{\max} \;\; \Phi^{\max}\right]^T , \qquad (1)$$

where $\Phi^{\max} = 2.9N$.

The forces in *me*- and *te*-tendon were estimated in each simulation. The forces in tendon for two first individual loadings were summarized and compared with the tendon forces, obtained when all for muscle forces were applied to the model at the same time. The difference between tendon forces, obtained

in simultaneous loading of the EM by all four muscles (third vector in (*1*)) and the sum of the tendon forces, obtained in each individual loading of the EM by extrinsic and intrinsic muscles (vectors one and two in (*1*)) characterizes the nonlinear («switching») behavior of the EM.

Study of the influence of the posture

Next, we studied how the force distribution among the tendons and the fingertip force change with the finger posture, and focused on the role of the intercrossing bands of the EM in these changes. To characterize the changes with the posture, the feasible tendon force set (FTFS) and feasible fingertip force set (FFS) were found (Valero-Cuevas et al., 2007).

The FTFS was calculated as set of all possible forces in the medial extensor tendon (*me,* 6 in Fig. 1) and the terminal extensor tendon (*te*, 10 in Fig. 1). These two tendons attaches the EM models to finger bones. To find a FTFS we applied all possible combinations of input muscle forces to the EM model:

$$\left[0\ 0\ 0\ 0\right]^T\ \left[\Phi^{\max}\ 0\ 0\ 0\right]^T\ \left[0\ \Phi^{\max}\ 0\ 0\right]^T\ \cdots\left[\Phi^{\max}\ \Phi^{\max}\ \Phi^{\max}\ \Phi^{\max}\right]^T, \quad (2)$$

Therefore, they may be 16 possible combinations of input forces. Each input force vector **Φ** gives a point in the plane of the forces in *me*- and *te*-tendon. An FTFS was characterized by a convex hull of these 16 points.

The similar approach was used to calculate an FFS. It was calculated as a set of all possible fingertip forces, that the fingertip can produced in all directions at the given maximal activation level of the muscles. To estimate an FFS we applied all possible combinations of input muscle forces to the EM, as in case of FTFS (2). Each input force vector **Φ** gives a point in 3D-space of x, y, z fingertip force components. The FFS was calculated as a convex hull of these 16 points.

Study of the influence of the activation level

We also studied how the FFS and FTFS changes when the forces of the muscle forces change. We compared an FTFS and a FFS of a full EM model when a normal force vector was used as a model input (all muscle forces of $\Phi^{\max} = 2.9N$), and when an input force vector was multiplied by a coefficient $\alpha = 0.5$, (all muscle forces of $\Phi = 1.5N$) :

$$\left[\Phi^{\max}\ \Phi^{\max}\ \Phi^{\max}\ \Phi^{\max}\right]^T\ \alpha\cdot\left[\Phi^{\max}\ \Phi^{\max}\ \Phi^{\max}\ \Phi^{\max}\right]^T. \quad (3)$$

Study of the influence of the lengths of the intercrossing bands

Finally, we studied how the lengths of the intercrossing fibers influence the force transmission. There were four fiber layers in the EM model: two interosseous medial fiber layers, radial and ulnar (shown in red in Fig. 1), and two extensor lateral fiber layers, radial and ulnar (shown in blue in Fig. 1) To study the influence of the lengths, the length of each fiber in one layer was multiplied by the same coefficient. We compared the initial case (drawing 2 in Fig. 2), the case when the interosseous medial fibers were shortened by 0.9 (drawing 1 in Fig. 2), and, finally, the case, when the extensor lateral fibers were shortened by 0.9 (drawing 3 in Fig. 2).

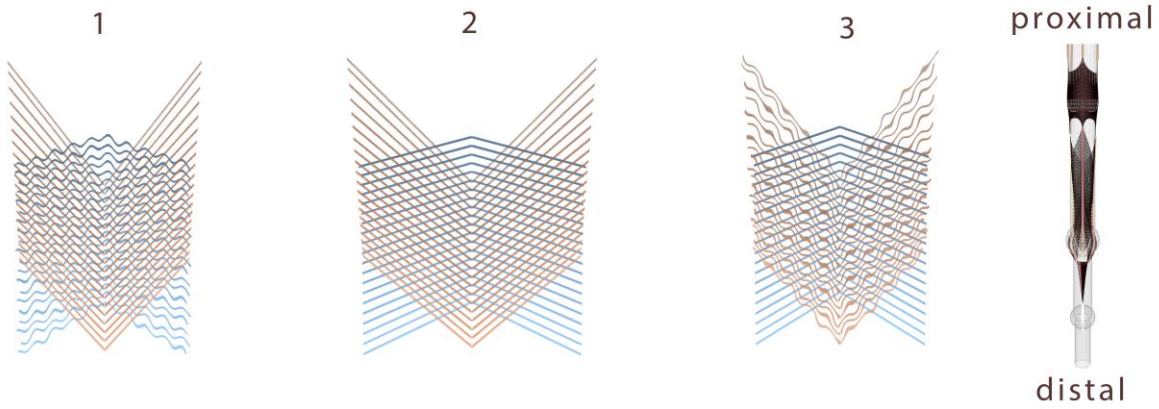

Fig. 2. The schematic view of the intercrossing fibers (1) when the interosseous medial fibers were shortened; (2) in initial state; (3) when the extensor lateral fibers were shortened.

Results

1. The linearity of the extensor mechanism with reference to the input forces

This section presents the study of the EM behavior linearity with reference to the input muscle forces. We firstly show how the forces, transmitted by the intercrossing fibers, *im* and *el*, depend on loading. The *im*-fibers transmit the force from interosseous muscles to me-tendon, and *el*-fibers transmits the force from extrinsic EDC muscle to lateral tendons and, as a result, to *te*-tendon. Fig. 3 shows how the forces of intrinsic muscles transmitted by ulnar *im*-fibers changes when the EDC muscle becomes active (Fig. 3a). Similarly, Fig. 3b shows how the forces of EDC transmitted by ulnar *el*-fibers changes when the intrinsic muscles become active.

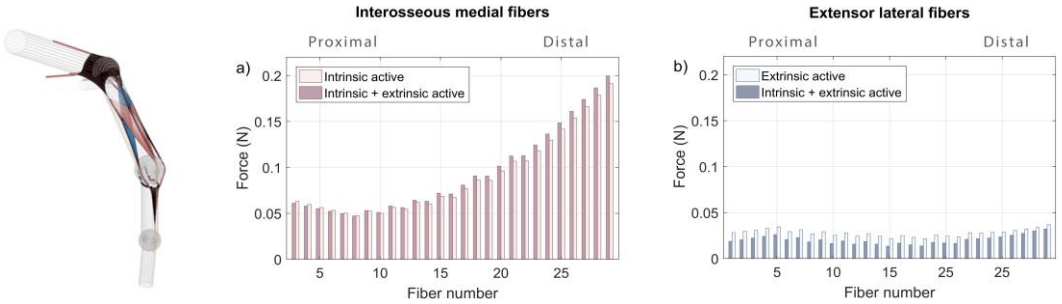

Fig. 3. (a) the forces in ulnar interosseous medial (im) fibers when only intrinsic muscles are active (light red bars) and when extrinsic EDC muscle is involved (dark red bars). (b) the forces in ulnar extensor lateral (el) fibers when only extrinsic EDC muscle is active (light blue bars) and when intrinsic muscles are also involved (dark blue bars).

The principal role of *im*-fibers is to transmit the forces from intrinsic muscles to the medial *me*-band, as well as the principal role of the *el*-finds is to transmit the forces from the extrinsic EDC muscle to lateral bands, which merge to form the terminal *te*-tendon. It is seen from the figure there is an influence of the EDC force on force transmission in *im*-fibers as well as the influence of the intrinsic muscle force on the force in *el*-fibers.

The force transmitted by the intercrossing fibers influence the forces in *me*- and *te*-tendon. Fig. 6 shows the study of the EM linearity concerning the forces in these tendons. The left column corresponds

to extended finger (MCP, PIP, DIP are 10°,10°,10°), middle column to mid-flexed finger (45°,45°,10°), and the last column corresponds to flexed finger (90°,90°,80°). The first row shows the forces produced in *me*-and *te*-tendons by application of the EDC muscle force the model, which is a extrinsic muscle. The second row shows the forces in tendons, obtained by application of the intrinsic muscle forces (UI, RI, LU) to the model. The third row shows the tendon forces when the forces from all four muscles are simultaneously applied (blue bars). The same figures shows the sum of the forces in tendons, created by individual application of the extrinsic and intrinsic muscle forces (violet bars). The differences between the blue and violet bars are related to nonlinear behavior of the extensor mechanism. Finally, the bottom row traces the differences between the blue and the violet rows.

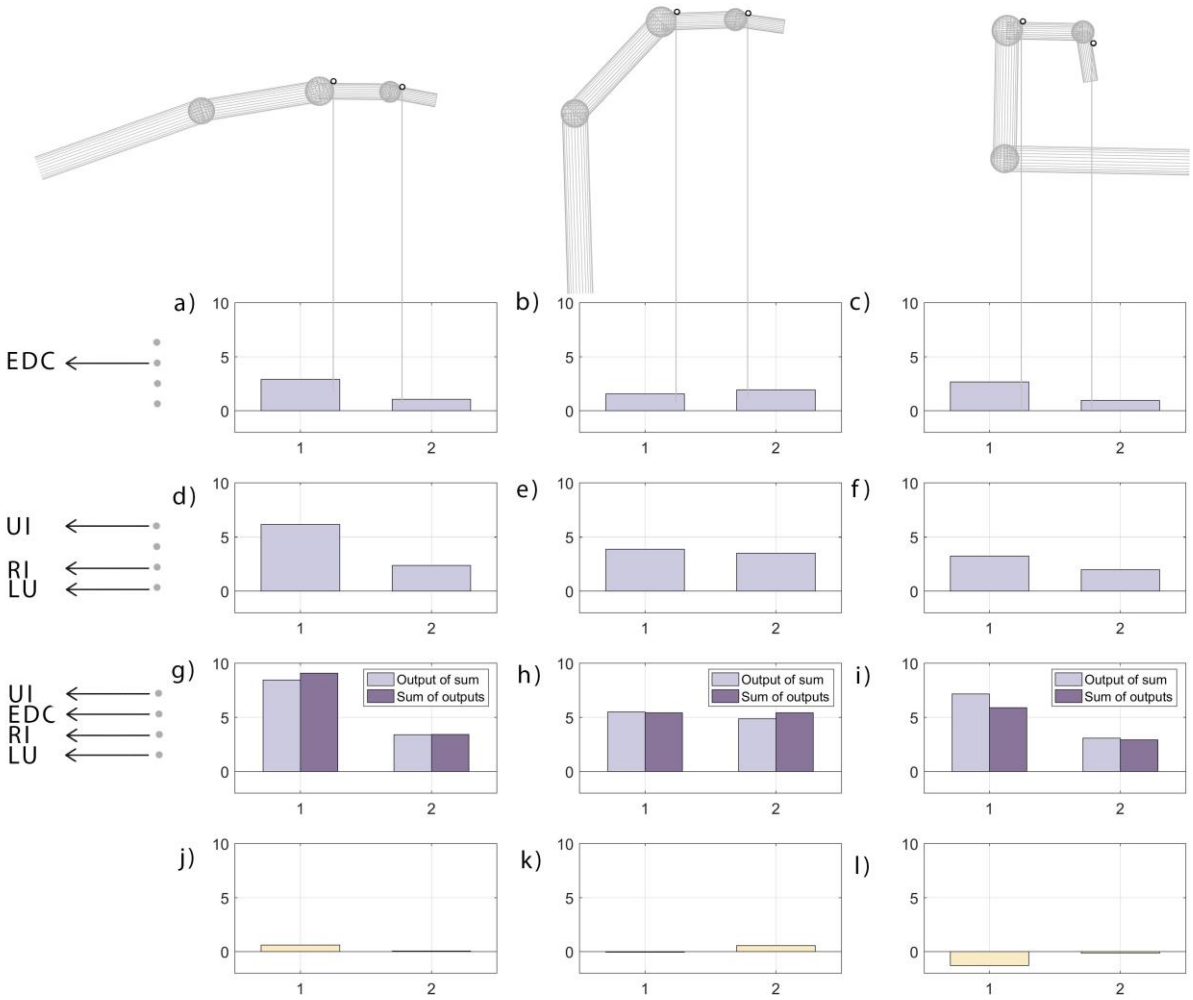

Fig. 4. The extensor mechanism model showing the non-linear behavior at different postures. The angles MCP,DIP,PIP are 10°,10°,10°for the left column; 45°,45°,10° for the central column; 90°,90°,80° for the right column. The first row (a-c) shows the forces in me and te-tendon when only extrinsic EDC force was applied to EM. The second row (d-f) shows the tendon forces when only intrinsic muscle (UI, RI and LU) forces were applied to EM. The third row (g-i) shows the tendon forces when all four muscle forces were simultaneously applied (blue). The same figures show the sum of the forces in tendons produced individually by extrinsic and intrinsic (violet). The difference between the tendon forces produced by simultaneous application of four muscle forces and the tendon forces, calculated as the sum of the tendon forces, produced individually by extrinsic and intrinsic muscles are due to the nonlinearity effect of the extensor mechanism. The fourth row shows the difference between the blue and violet columns tendon forces.

It may be seen from the figure that the full EM model shows the nonlinear behavior. For example, for the EM of the finger in midflexion, the difference between the tendon forces when all muscle forces were applied simultaneously and the tendon forces, calculated as the sum of the results of individual intrinsic and extrinsic muscle force application, were -0.06 N and 0.56 N for *me*- and *te*-tendon correspondingly. These values are 11.6% and -1.0% of the force in these tendons when all muscle forces were applied.

On the contrary, the trivial EM model does not show such a behavior. For example, for a trivial EM model in midflexion, the difference between the tendon forces when all muscle forces were applied simultaneously and the tendon forces, calculated as the sum of the results of individual intrinsic and extrinsic muscle force application were $0.2 \cdot 10^{-6}$ N and $0.7 \cdot 10^{-6}$ N for *me*- and *te*-tendon correspondingly. This difference are related to computational error.

The influence of the posture on a feasible tendon set and feasible force set.

The changes of the posture result in the changes of the force distribution among the extensor mechanism bands, tendon moment arms and the finger Jacobian.

Fig. 5 shows the force distribution among the EM intercrossing fibers with the posture.

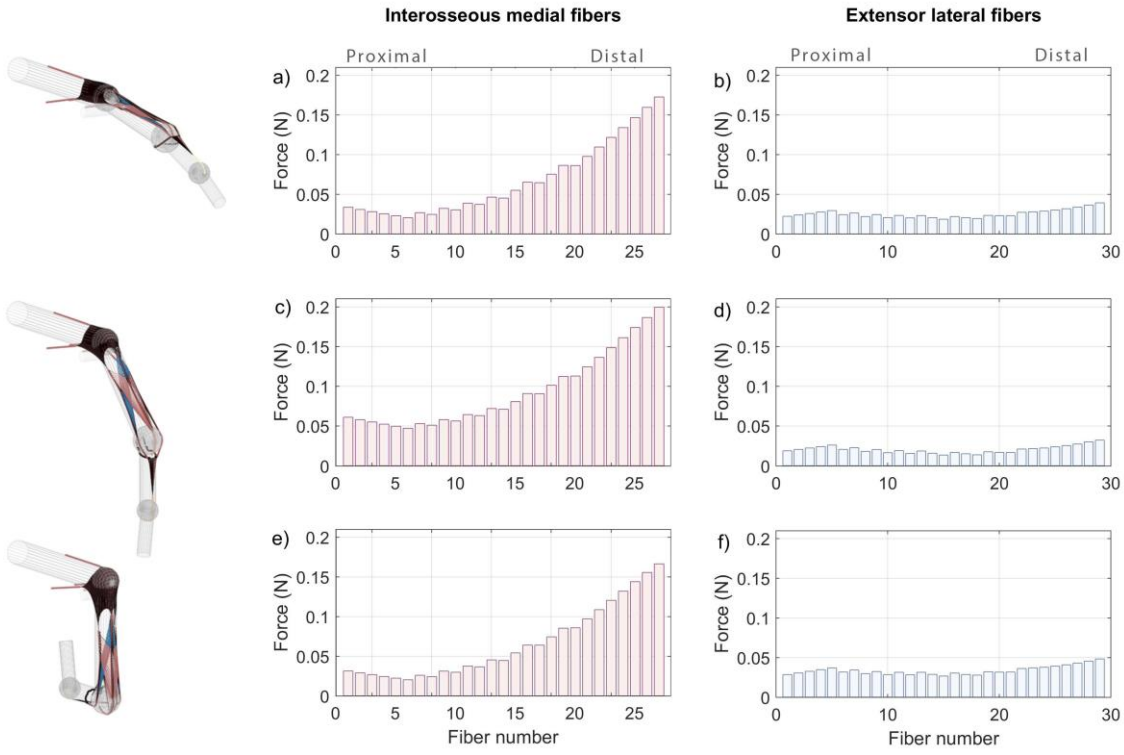

Fig. 5. The forces in intercrossing fibers for three postures (red: interosseous medial fibers; blue: extensor lateral fibers).

The extensor mechanism is principally attached to bones by two tendons: medial extensor tendon and terminal extensor tendon. All bands of the extensor mechanism are coupled either with the former or latter tendon. Hence, the change of the force distribution among the extensor mechanism bands changes the ratio between the forces in these tendons.

Each combination of the input muscle forces correspond to a combination of forces in terminal and medial extensor tendon, forming the feasible tendon force set (FTFS). Fig. 6 shows how the FFTS changes with the posture.

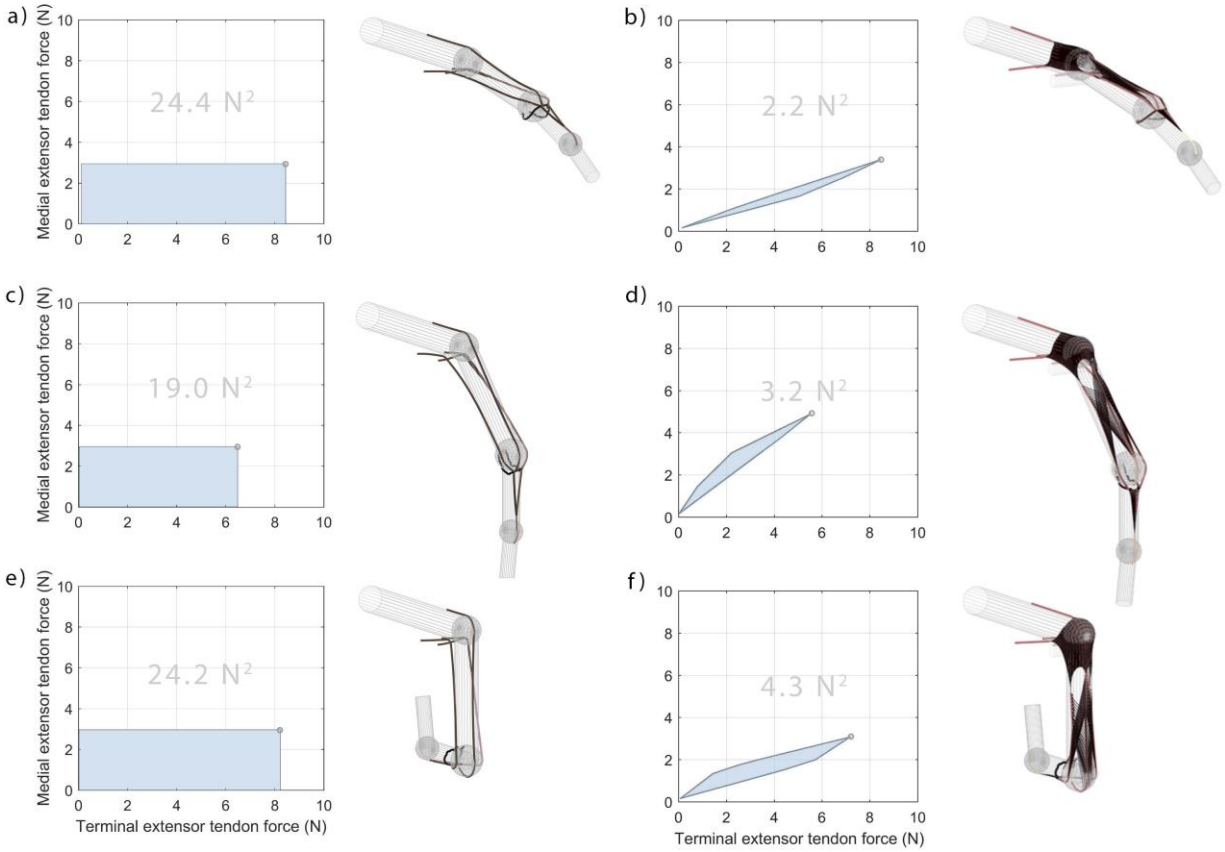

Fig. 6. The changes of the FTFS with posture. Left column corresponds to a trivial extensor mexanism model, right collumn corresponds to a full model. The peak force which corresponds to loading of the EM models by all four muscles, is shown by a circle in each FTFS,. The area of each FTFS is also indicated

It can be seen from the left column of the image, that the FTFS in the trivial model has a rectangular shape for all postures, because there is no influence of the intrinsic muscles on the medial extensor tendon and, similarly, no influence of the EDC extensor on terminal extensor tendon. The area of rectangular is smaller for mid-flexion posture that may be explained by stretching of the triangular membrane.

The right column shows changes of the FTFS in the full model with posture. It can be noticed that the area of the FTFSs of the full model is lower than the area of the FTFSs for the trivial model (*e.g.* 2.2 N^2 vs 24.4 $N^2$for the extended finger). This decrease of the FTFS area may be explained by the fact

that in trivial model, the force in each of two attachment tendons, *me* and *te*, are controlled independently, ensuring the highest possible FTFS area. In the full EM model, the forces in these tendons are dependent, reducing the FTFS area. The changes of the shape and the orientation of the full model's FTFS with posture illustrate the variation of the force transmission among the tendons with the posture. The orientation variation may be quantified by the ratio between the forces in *me*- and *te*-tendon in the EM loaded by all four muscles (peak force, shown by circle in the figure). It is seen from the figure that the *me:te* force is higher in the full EM model with the higherst value of 0.89 for the mid-flexed finger (d). The *me:te* vales for both models in all postures are listed in Table 1.

The changes of the tendon forces, among the changes of the tendons' moment arms and finger Jacobian results in changes of the fingertip force with posture. Fig. 7 shows how the changes in the effects of the posture on xOy projections of the FFS. The left column corresponds to a trivial EM model, the right column to the full EM model. The dark blue area corresponds to the forces created only by the muscles, attached to the extensor mechanism (UI, EDC, RI, and LU) and with no forces in flexor muscles. The light area stands for the forces, created when the flexor muscles were also active (*flexor digitorum profundus, flexor digitorum superficialis*).

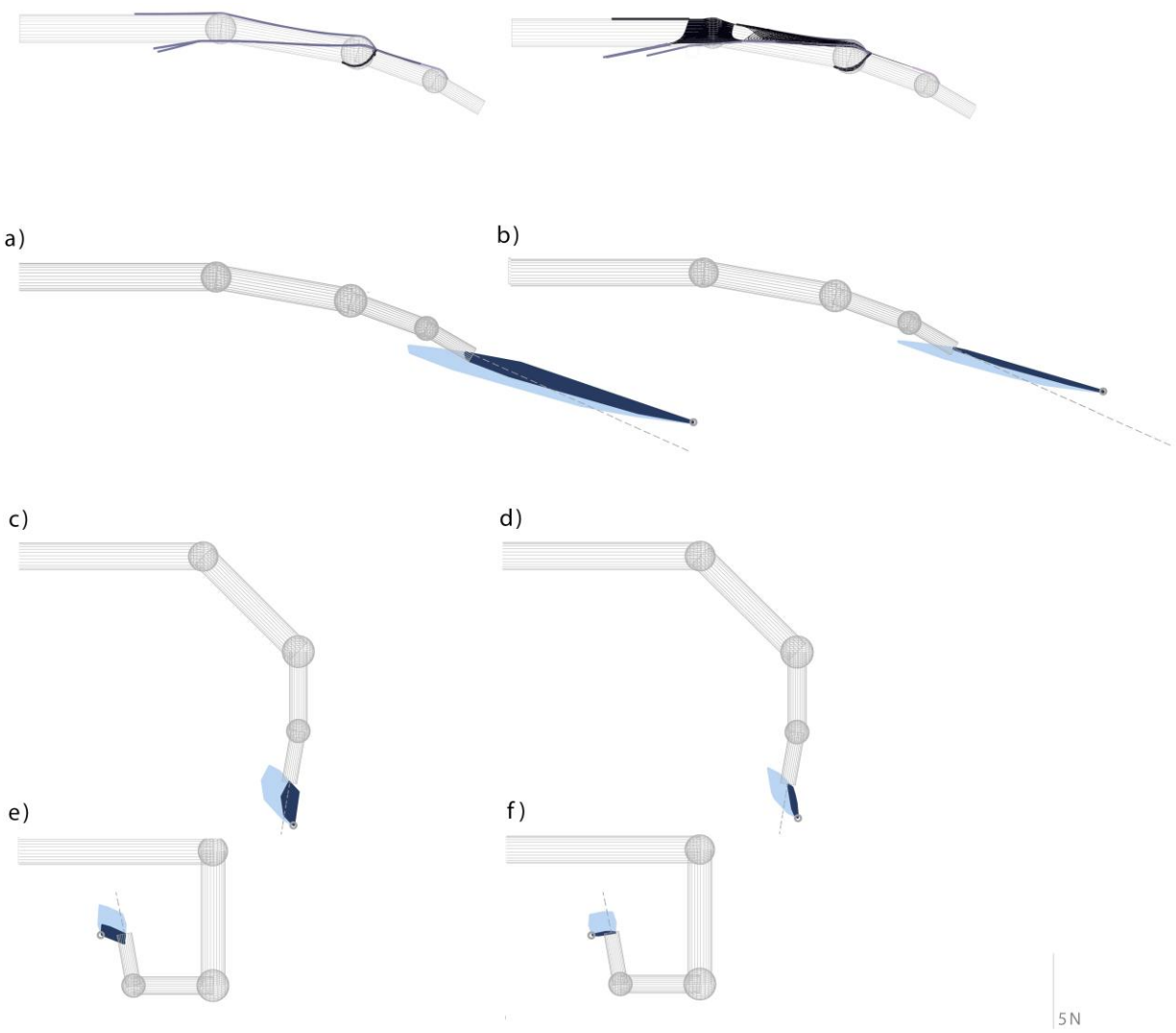

Fig. 7. Projection of the feasible force set for different postures: a) extension posture (MCP = 10°,PIP = 10°; DIP = 10°), b) mid-flexion posture (MCP = 45°,PIP = 45°; DIP = 10°), c) flexion posture (MCP = 90°,PIP = 90°; DIP = 80°).

The changes of the FFS of the trivial model are related mostly to the changes of the finger Jacobian and the tendon's moment arms with posture. The FFS changes of the full EM model are related also to the changes of the force distribution among the tendons. It is seen from the figure that the area of the FFS of the trivial model is higher than the area of the FFS of the full EM model. It corresponds to the fact that the area of the FTFS of the membrane model is lower than the area of the FTFS of the trivial model. The changes of the FFS orientation were characterized by the angle between the peak force (shown by circle) and the axis of the third phalanx (shown by the dashed line). The angles for other postures are listed in Table 1 for the both trivial and full model.

Table 1. The me:te-tendon force ratios and the angle of the peak force with reference to the third phalanx bone for three postures

Posture	**The tendon /force ratio *me:te* (a.u.)**		**The peak force angle**	
	Trivial model	Full model	Trivial model	Full model

Extension	0.35	0.40	13.0°	13.9°
Mid-flexion	0.46	0.89	16.1°	26.3°
Flexion	0.36	0.43	81.2°	88.7°

It is seen from the table that the *me:te* ratios are higher for the full EM model, in which the interosseous muscle also contributes to *me*-tendon force. It can be noticed that the angle between the third phalanx axis and the peak force depends on the *me:te* ratio. Therefore, this angle is higher for the full EM model than for the trivial one with the highest value for the mid-flexed finger.

2. The influence of the activation level on the fingertip force

Next, the influence of the muscle activation on both FTFS and FFS was studied. We analyzed the variation of the FFS of the full EM model for two different force levels: normal, when all muscles forces were 2.9 N and low level, when all muscle forces were of 1.5 N. Fig. 8 shows the FTFS and FFS (left and right column correspondingly) of the full EM model for two force levels. For simplicity, only the part of the FFS created by EM muscles (UI, EDC, RI, and LU) is shown.

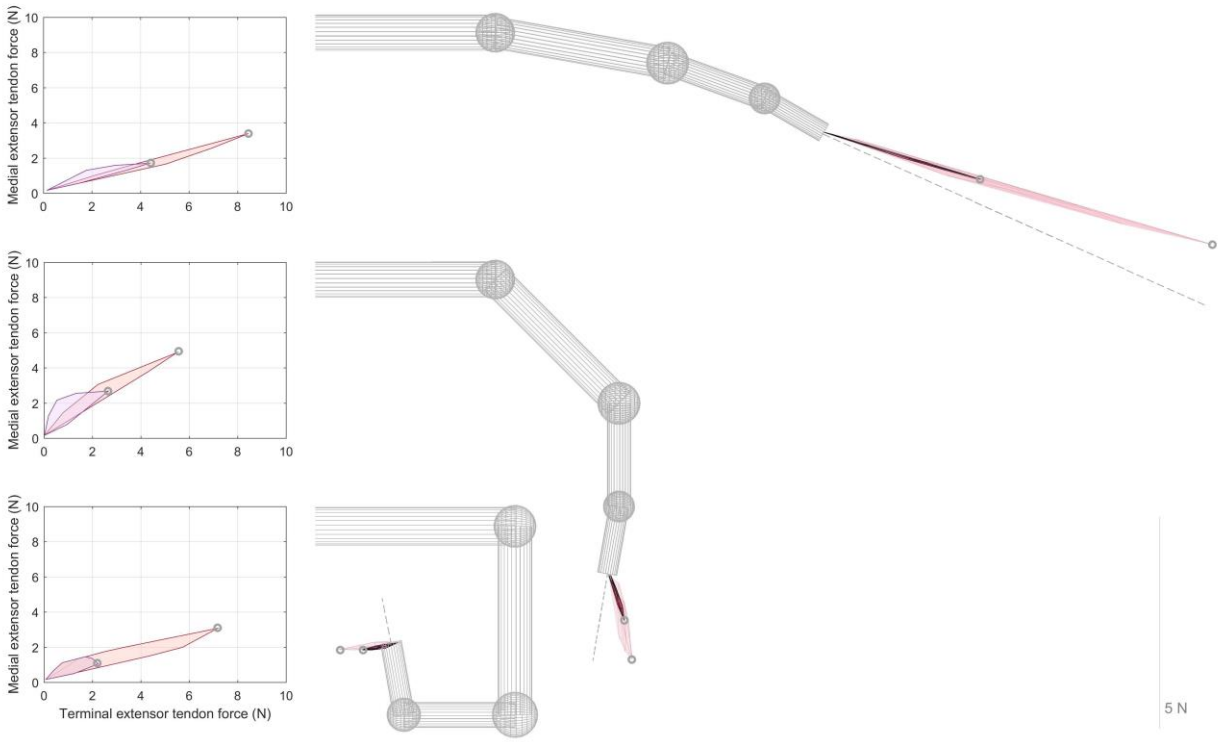

Fig. 8. The FTFS and FFS of the full EM model for different postures and different muscle activation level, normal (red) and low (violet). Only the part of the FFS created by EM muscles (UI, EDC, RI, LU) is shown.

It may be seen from the figure that the area of the FTFS and FFS increases with muscle activation level. Moreover, the increase of the muscle activation level also slightly affects the shape of the FTFS and FFS and their orientation. For example, for the mid-flexed finger this ratio is 1.00 for the low force level

vs 0.89 for normal activation level. These changes of the shape may be explained by slight deformations of the EM with force level. The changes of the of the FTFSs causes in changes of the FFS force and orientation. For example, for the same posture the angle between the peak force and the axis of the third phalanx was 29.7° for the low force level vs 26.3° for normal activation level. The *me:te* ratios and the peak force angles for other postures are listed in Table 2.

Table 2. The me:te-tendon force ratios and the angle of the peak force with reference to the third phalanx bone for two force levels.

Posture	**The tendon /force ratio *me:te* (a.u.)**		**The peak force angle**	
	Low force level	Normal force level	Low force level	Normal force level
Extension	0.39	0.40	13.4°	13.9°
Mid-flexion	1.00	0.89	29.7°	26.3°
Flexion	0.67	0.43	101.8°	88.7°

It can be seen from the figure that for mid-flexed and flexed finger the *me:te* ratio is higher for the low force level. Consequently, in these postures, the peak force angle is higher at low force.

3. The influence of the parameters on the fingertip force

Finally, we studied how the FTFS and FFS changes with model parameters, which were the length of the intercrossing fibers. We compared the full EM model with three different length of intercrossing fibers, as shown in the “Methods” section. The FTFSs and FFSs for these three cases are shown in Fig. 9. For simplicity, only the part of the FFS created by EM muscles (UI, EDC, RI, and LU) is shown.

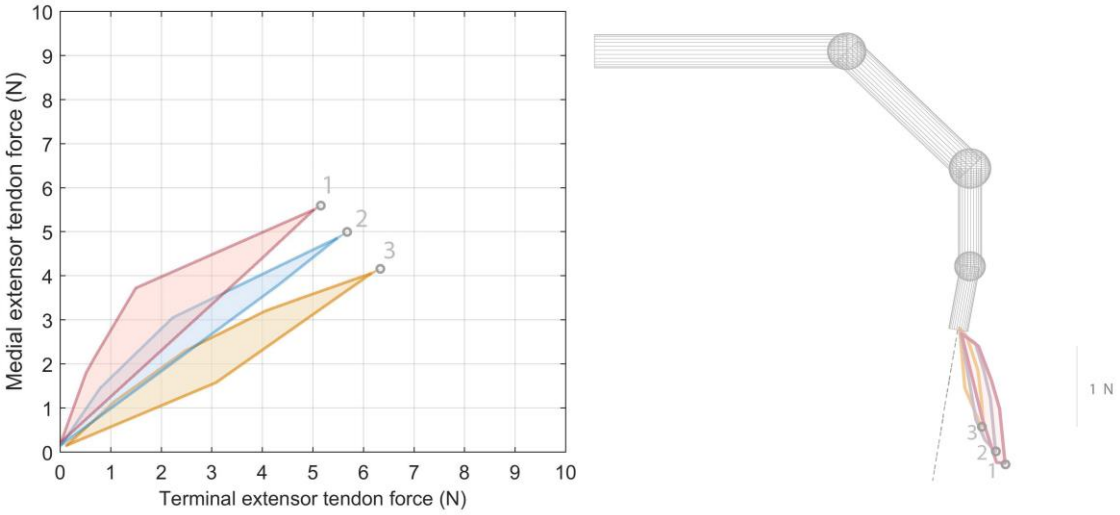

Fig. 9. The influence of the fiber length on the FTFS and FFS. 1: interosseous medial fibers shortened; 2: initial state; 3: extensor lateral fibers shortened. Only the part of the FFS created by EM muscles (UI, EDC, RI, LU) is shown.

It may noticed that shortening of the interosseous medial fibers increases the force in *me*-tendon, while shortening of the extensor later fibers increases the force in *te*-tendon. The ratio of the *me*-tendon force to the *te*-tendon force were 1.10 for the case where the interosseous medial fibers were shortened (1); 0.89 for the initial case (2), and 0.67 for the case where the extensor lateral fibers were shortened (3). These results illustrates the fact that the interosseous bands connect the interosseous muscle with the *me*-tendon, and their shortening increases the fraction of the force transmitted to the me-tendon. Vice versa, the extensor later fibers connect the EDC muscle with the *te*-tendon, and shortening of theses fibers increases the force in the later. The changes of FFS cases the following changes of FFS: the angle between the third phalanx axis and the peak force was 28.5° for the case (1), 26.3° for the case (2), and 24.1° for the case (3). Table 3 summarizes the changes of the FTFS and FFS with the intercrossing fiber length.

Table 3. The me:te-tendon force ratios and the angle of the peak force with reference to the third phalanx bone for three cases of intercrossing fiber lengths.

Posture	**The tendon /force ratio *me:te* (a.u.)**			**The peak force angle**		
	im-fibers shortened	Initial	*el*-fibers shortened	*im*-fibers shortened	Initial	*el*-fibers shortened
Mid-flexion	1.10	0.89	0.67	28.5°	26.3°	24.1°

Discussion

In this work, we proposed a numeric EM simulator and created a precise model of the extensor mechanism (the full model). This model takes into account the intercrossing fibers of the extensor mechanism and includes the extensor hood and triangular ligament, modeled as membranes. The models

incorporates the transverse retinacular ligament as well. To study the role of the intercrossing bands, the full model was compared with trivial model with no structures, connecting the lateral and medial band.

The role of the intercrossing fibers

We firstly demonstrated that the EM shows nonlinear behavior with respect to input muscle forces. These results conform the findings of (Valero-Cuevas et al., 2007). This phenomenon may be partially explained by modifications of the force transmission by intercrossing fibers and partially by force transmission in the extensor hood.

Secondly, we showed how the forces in intercrossing fibers changes with posture and how this modifies the force distribution in medial and terminal extensor tendon *me* and *te*. The postural variation of the forces in these two bands results in changes of the feasible tendon force set FTFS and feasible fingertip force set FFS. The FTFS and FFS postural variations of the full EM model were presented and compared with the FTFS and FFS of the trivial model with no intercrossing bands. The areas of FTFSs and FFSs of the full EM model is significantly lower of the areas of FTFSs and FFSs, produced by the trivial model. This area increase is due to the fact that the trivial EM model enables the independent control of the forces in the *me*- and *te*-tendon. However, in the case of the EM with the intercrossing bands these forces are mutually dependent. Although this dependency between the forces in *me*- and *te*-tendons reduces the FFS area of the finger it may simplify the finger control.

Thirdly, we shown how the fore activation level changes the FTFS and the FFS. It was shown that among with increase of the FTFS and FFS areas with the muscle activation level, the shape and the orientation of the force sets slightly changes because of the deformation of the structures, connecting the medial and lateral bands.

Finally, we shown how the parameters of the intercrossing fibers influence the force transmission in the EM. It was demonstrated that for the full EM-model, loaded with identical forces for all muscles, the in *me*-tendon increases with shortening of the interosseous medial fibers, and the force in *te*-tendon increases with shortening of the extensor later fibers.

Limitations and perspectives

The model has several limitations. Firstly, the model topology oversimplifies the real EM anatomy, Over MCP joint the EM was represented only by the extensor hood. However, the metacarpophalangeal fibrous griddle, or sagittal band, which connect the extensor tendons to the deep transverse intermetacarpal ligament and capsular joint (Zancolli, 1979) was not taken into account. Moreover, no attachments of the EM at the base of the proximal phalanx were taken into account. Secondly, the bones were modeled as cylinders with spheres corresponding to the joints. Although this assumptions may result in reducing the fingertip force predicted by the model and may limit the model application for the medical application, e.g. the surgical planning, the purpose of the current work was to shown how the intercrossing fibers can influence force transmission among the EM bands.

As a future work, the cadaveric studies may be carried to validate the role of the EM-intercrossing fibers. Moreover, more complicated model of the extensor hood may be proposed and the force transmission in it may be studied.

Acknowledgements

The work was supported by IDEX scholarship for international mobility. The authors would like to acknowledge the USC intern student Vishweshwer Shastri for his participation in the extensor mechanism modelling. The authors would also like to acknowledge Gelu Ionescu†, an engineer in GIPSA-Lab, for his assistance with the programming of the extensor mechanism simulator.

References

Dogadov, A., Alamir, M., Serviere, C., Quaine, F., 2017. The biomechanical model of the long finger extensor mechanism and its parametric identification. J. Biomech. 58. doi:10.1016/j.jbiomech.2017.04.030

Garcia-Elias, M., An, K.N., Berglund, L., Linscheid, R.L., Cooney, W.P., Chao, E.Y., 1991. Extensor mechanism of the fingers. I. A quantitative geometric study. J. Hand Surg. Am. 16, 1130–1136. doi:10.1016/S0363-5023(10)80079-6

Harris, C., Rutledge, G.L., 1972. The functional anatomy of the extensor mechanism of the finger. J. Bone Joint Surg. Am. 54, 713–726. doi:10.1097/00006534-197301000-00039

Hu, D., Ren, L., Howard, D., Zong, C., 2014. Biomechanical Analysis of Force Distribution in Human Finger Extensor Mechanisms. Biomed Res. Int. 2014.

Landsmeer, J.M.F., 1949. The anatomy of the dorsal aponeurosis of the human finger and its functional significance. Anat. Rec. 104, 31–44. doi:10.1002/ar.1091040105

Lee, S.W., Chen, H., Towles, J.D., Kamper, D.G., 2008. Effect of finger posture on the tendon force distribution within the finger extensor mechanism. J. Biomech. Eng. 130, 051014. doi:10.1115/1.2978983

Leijnse, J.N. a L., Spoor, C.W., 2012. Reverse engineering finger extensor apparatus morphology from measured coupled interphalangeal joint angle trajectories - a generic 2D kinematic model. J. Biomech. 45, 569–578. doi:10.1016/j.jbiomech.2011.11.002

Sachdeva, P., Sueda, S., Bradley, S., Fain, M., Pai, D.K., 2015. Biomechanical simulation and control of hands and tendinous systems. ACM Trans. Graph. 34, 42:1–42:10. doi:10.1145/2766987

Sarrafian, S.K., Kazarian, L.E., Topouzian, L.K., Sarrafian, V.K., Siegelman, A., 1970. Strain variation in the components of the extensor apparatus of the finger during flexion and extension. A biomechanical study. J. Bone Joint Surg. Am. 52, 980–990.

Schultz, R., Furlong II, J., Storace, A., 1981. Detailed anatomy of the extensor mechanism at the proximal aspect of the finger. J. Hand Surg. Am. 6, 493–498. doi:7276481

Stack, H.G., 1963. A study of muscle function in the fingers. Ann. R. Coll. Surg. Engl. 33, 307–322.

Synek, A., Pahr, D.H., 2016. The effect of the extensor mechanism on maximum isometric fingertip forces: A numerical study on the index finger. J. Biomech. 49, 3423–3429. doi:10.1016/j.jbiomech.2016.09.004

Valero-Cuevas, F.J., 2015. Fundamentals of Neuromechanics, Biosystems & Biorobotics. Springer London, London. doi:10.1007/978-1-4471-6747-1

Valero-Cuevas, F.J., Yi, J.W., Brown, D., McNamara, R. V., Paul, C., Lipson, H., 2007. The tendon network of the fingers performs anatomical computation at a macroscopic scale. IEEE Trans. Biomed. Eng. 54, 1161–1166. doi:10.1109/TBME.2006.889200

Van Zwieten, K.J., 1980. Some functional-anatomical characteristics of finger movements in the hands of human and other primates 518–528.

Vaz, A., Singh, K., Dauphin-Tanguy, G., 2015. Bond graph model of extensor mechanism of finger based on hook–string mechanism. Mech. Mach. Theory 91, 187–208. doi:10.1016/j.mechmachtheory.2015.03.011

Zancolli, E., 1979. Structural and Dynamic Bases of Hand Surgery. J.B. Lippincott Company, Philadelphia; Toronto.